The crossover from a ferroelectric to a relaxor state in lead-free solid solutions

Annie Simon, Jean Ravez and Mario Maglione

ICMCB—CNRS, 87 avenue A Schweitzer, 33608 Pessac, France

Abstract
We investigate the gradual crossover from ferroelectric to relaxor behaviour
versus substitution in lead-free ceramics. We show that the Vogel–Fulcher law
in the relaxor state is the extrapolation of the ferroelectric line. To explain this
extrapolation, we suggest that both the host matrix and the impurity induced
clusters are triggered by the $BaTiO_3$ soft mode correlation length. The Ti–O
bond oscillations are the key mechanism.

1. Introduction

Ferroelectric materials, mainly of perovskite type, may be divided in two different classes
according to their behaviour: depending on whether they are classical ferroelectrics or
relaxors [1].

Here are some well-known examples of the perovskite ABO_3 type:

- classical ferroelectrics: $KNbO_3$, $BaTiO_3$ (BT), $PbTiO_3$, . . .,
- relaxors: $Pb(Mg_{1/3}Nb_{2/3})O_3$ (PMN), $Pb(Sc_{1/2}Ta_{1/2})O_3$ (PST), $Pb(In_{1/2}Nb_{1/2})O_3$ (PIN), PLZT, ...

In addition to having the usual applications of ferroelectric materials, relaxors are of great
interest as dielectrics for use in capacitors and actuators [2].

Most relaxors are lead-based ceramics such as PMN and derived compounds, or
$Pb(M'_{1/2}M''_{1/2})O_3$ with long range polar order. Electron microscopy and diffuse x-ray scattering
evidenced ordered nanoregions, for example 1Mg:1Nb for PMN.

However, these compositions have the obvious drawbacks associated with the volatility
and toxicity of PbO. Therefore, much current research is directed towards more environment-
friendly Pb-free relaxor materials [3]. To date, similar studies on lead-free perovskite
ceramics have not yet allowed us to clearly establish such nanostructure. The lead-free
compositions studied were derived from $BaTiO_3$ by cationic homovalent substitutions
$(Ba(Ti_{1-x}M_x)O_3$ (M = Zr, Sn, Ce), $Ba_{1-x}Ca_x(Ti_{1-x}Zr_x)O_3)$ [3, 4] or heterovalent substi-
tutions $(Ba_{1-x}K_{x/2}La_{x/2}TiO_3$, $Ba_{1-x}A_{2x/3}\square_{x/3}TiO_3$ (A = La, Bi), $Ba_{1-x/2}\square_{x/2}(Ti_{1-x}M_x)$

O_3 (M = Nb, Ta), $Ba_{1-x}K_x(Ti_{1-x}M_x)O_3$ (M = Nb, Ta), $Ba_{1-x}Na_x(Ti_{1-x}Nb_x)O_3$, $Ba(Ti_{1-x}Li_x)O_{3-3x}F_{3x}$, $Ba_{1-x}K_x(Ti_{1-x}Mg_x)O_{3-3x}F_x$ [5–10]).

The aim of the present work is to determine the crossover from ferroelectric to relaxor behaviour versus substitution rate in lead-free ceramics. The continuous change from ferroelectric to relaxor behaviour is a unique feature of lead-free solid solutions. In lead-containing compounds, only well-defined compositions lead to a relaxor low temperature state. In addition, the exact nature of the relaxor state in lead-free perovskites is still a matter of debate [11]. Investigating the gradual change from ferroelectric to relaxor behaviour is thus helpful for understanding the physics of the latter. One hopes that this would also help in understanding lead-free relaxors, which still raise a number of unsolved questions. To this end, we will focus on the following compositions: $Ba(Ti_{1-x}Zr_x)O_3$, $Ba_{1-x/2}\square_{x/2}(Ti_{1-x}Nb_x)O_3$, $Ba_{0.95x}\square_{0.05x}(Ti_{0.90}Nb_{0.10})O_{2.05+0.95x}$ and $Ba(Ti_{1-x}Li_x)O_{3-3x}F_{3x}$ belonging to the various systems $BaO-TiO_2-ZrO_2$, $BaO-TiO_2-Nb_2O_5$ and $BaO-BaF_2-TiO_2-LiF$ [3, 7, 9, 12].

We thus have homovalent and/or heterovalent cationic substitutions at six CN sites, anionic substitutions and also non-stoichiometric compositions.

2. Experimental details

The various compositions were obtained from carbonates, oxides and fluorides after calcination at temperatures between 1100 and 1200 °C for 15 h under oxygen. Disc-shaped ceramics were sintered at 1250–1400 °C, depending on the composition, for 4 h under an oxygen atmosphere. Oxyfluorides were prepared in platinum sealed tubes to prevent hydrolysis.

Powder x-ray diffraction made it possible to determine the limits of the perovskite solid solution domains close to BT. The diameter shrinkages $\Delta\Phi/\Phi$ (($\Phi_{init} - \Phi_{fin})/\Phi_{init}$) of the ceramics are in the range 14–16%. The densities of the sintered samples were 90–93% of the theoretical values. No sintering additives were used. From room temperature x-ray scattering, we checked that all ceramics were single phased and free from unwanted defects.

Dielectric measurements were performed on ceramic discs after deposition of gold electrodes on the circular faces by dc sputtering. The real and imaginary parts of the permittivity ε'_r and ε''_r were measured under helium as a function of both temperature (77–500 K) and frequency (10^2–2×10^5 Hz) using a Wayne-Kerr 6425 component analyser. The values of the Curie temperature T_C, the temperature of the ferroelectric–paraelectric transition, and of T_m, at which ε'_r versus (T, f) shows a maximum, for the relaxor compositions were determined. It has been found that in many relaxors the relationship between the frequency f of the ac measurement field and the temperature T_m can be described using the Vogel–Fulcher (VF) relationship:

$$\log f = \log f_0 - E_a/(k(T_m - T_{VF})) \tag{1}$$

where f_0 is the Debye frequency, T_m is the temperature of the dielectric maximum at the given frequency f, T_{VF} is the static freezing temperature, E_a is the activation energy and k is the Boltzmann constant [13, 14]. On the relaxor side of our phase diagram, we fitted all the dielectric data to this Vogel–Fulcher equation.

3. Results

Whatever the system, the ferroelectric state remained for compositions close to $BaTiO_3$ with a lowering of T_C from $T_C = 400$ K ($BaTiO_3$). Beyond a definite substitution rate x, ceramics have relaxor properties. Figures 1 and 2 show, as examples, the dielectric behaviour difference between the ferroelectric state and the relaxor one, for compositions
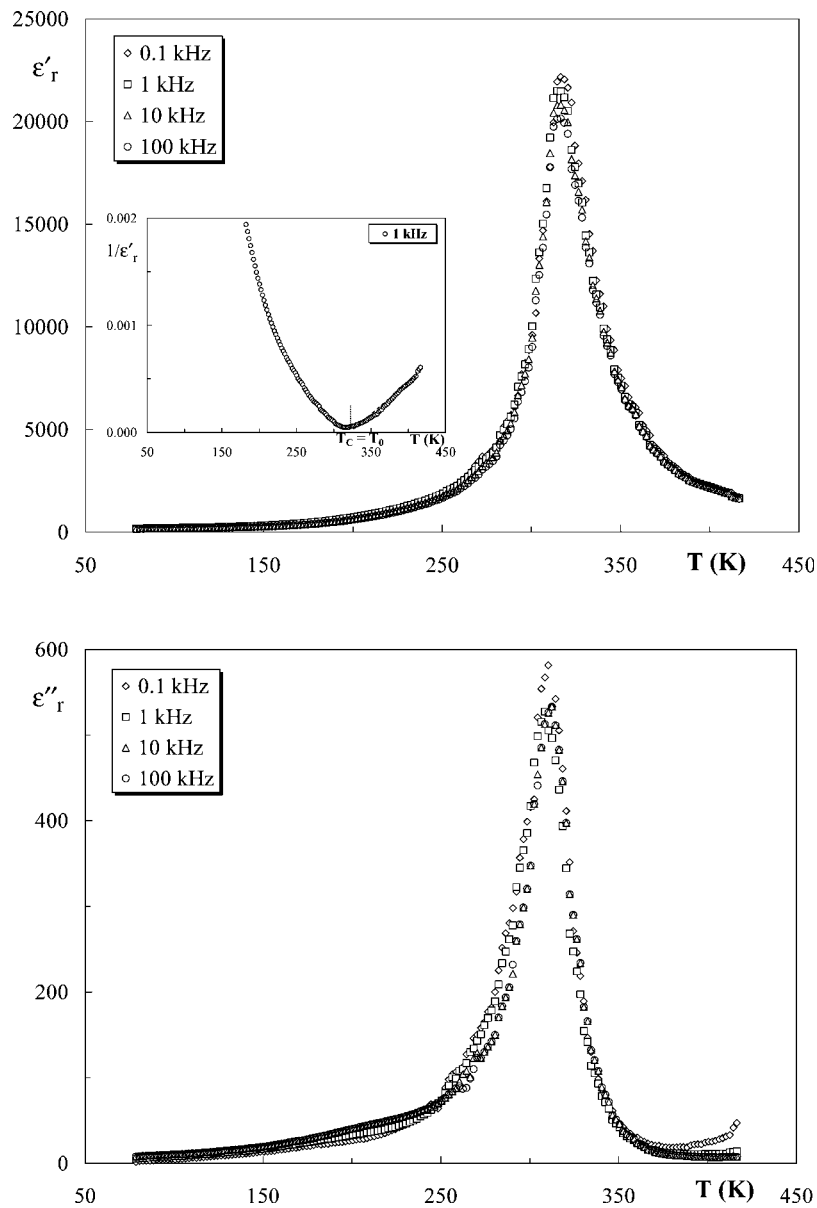
Figure 1. Temperature and frequency dependences of ε'_r and ε''_r, the real and imaginary parts of the permittivity, and the temperature dependence of $1/\varepsilon'_r$, for a ceramic with the composition $Ba(Ti_{0.80}Zr_{0.20})O_3$.

belonging to the $Ba(Ti_{1-x}Zr_x)O_3$ system. For a composition corresponding to $x = 0.20$, there was only one slightly broad peak of ε'_r which occurred at the ferroelectric–paraelectric temperature. The temperature dependence of $1/\varepsilon'_r$ showed that the Curie–Weiss law $\varepsilon'_r = C/(T - T_0)$ is followed and that the ferroelectric transition is of second order, since the transition temperature T_C and the Curie temperature T_0 are the same. For a composition corresponding to $x = 0.35$, the peak of ε'_r became very broad with frequency
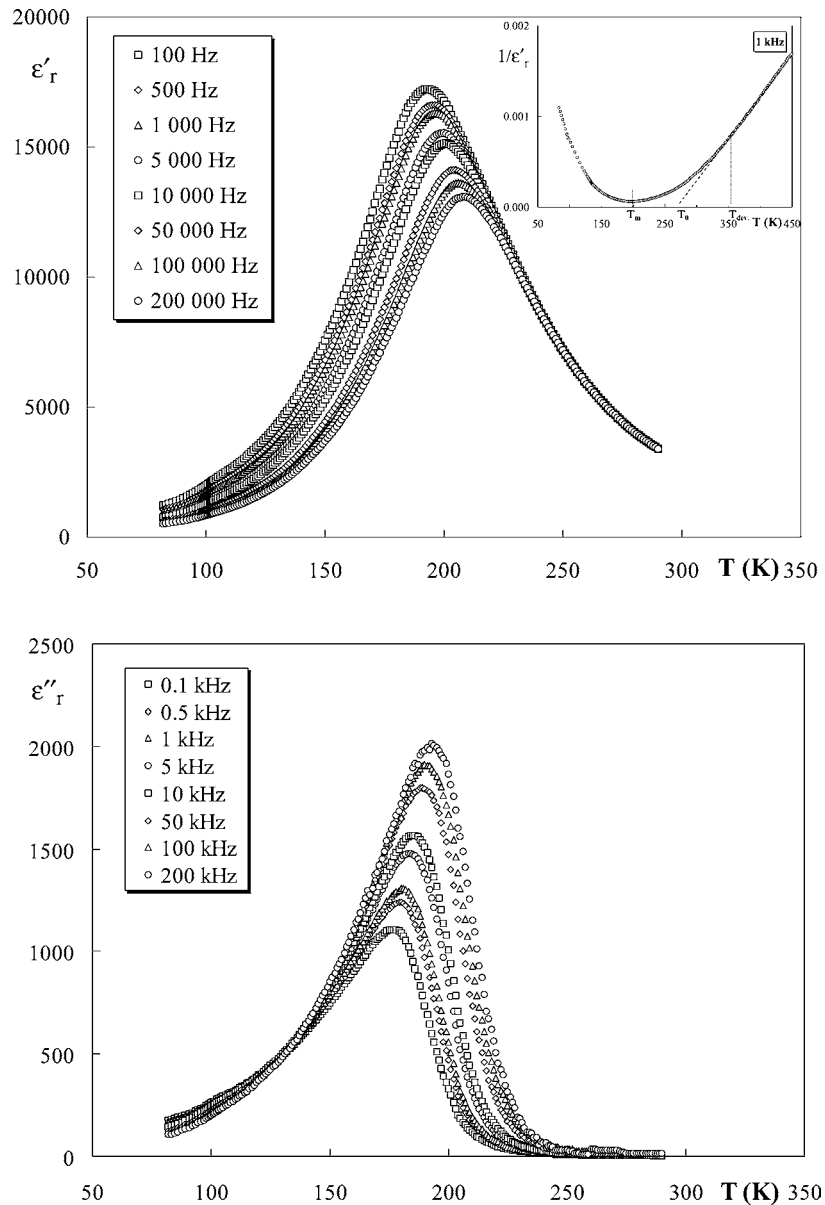
Figure 2. Temperature and frequency dependences of ε'_r and ε''_r, the real and imaginary parts of the permittivity, and the temperature dependence of $1/\varepsilon'_r$, for a ceramic with the composition $Ba(Ti_{0.65}Zr_{0.35})O_3$.

dispersion of ε'_r and ε''_r and shift of T_m. The temperature T_m of the maximum of ε'_r was shifted to higher values as the frequencies increased. A frequency dispersion sets in near T_m, the value of ε'_r decreasing when the frequency increases. The temperature and frequency variations of the imaginary part ε''_r of the permittivity were also specific to a relaxor behaviour: the temperature T_m of the ε''_r maximum was shifted to higher values at greater frequencies, but in contrast to the evolution of ε'_r, ε''_r increased when the frequency
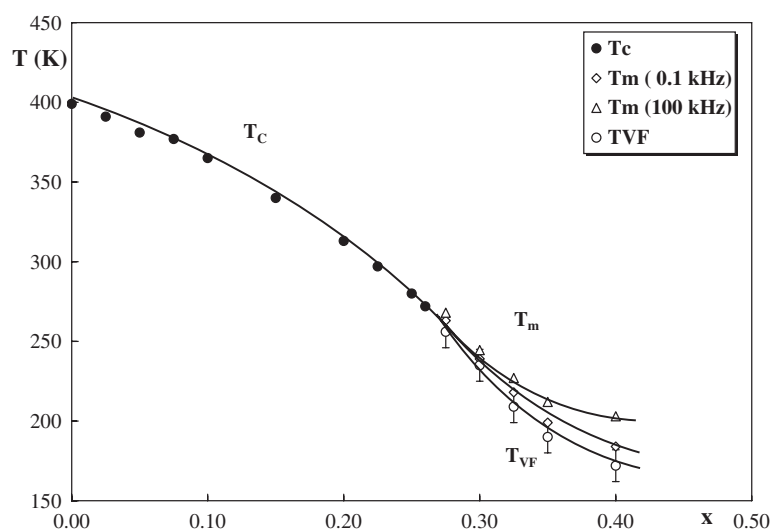
Figure 3. Variations of the transition temperatures T_C, T_m and T_{VF} with composition for ceramics of the $Ba(Ti_{1-x}Zr_x)O_3$ system.

increased. In addition, there was a deviation from the Curie–Weiss law. The value of the Curie–Weiss temperature T_0 was greater than that of T_m. All these dielectric characteristics are typical of relaxor behaviour. As x increased, the value of $T_{dev} - T_m$ also increased, implying that the relaxor effect also increased.

When the local strength of the substituted defects increases, the ferroelectric–relaxor crossover composition x_{f-r} decreases:

- for the homovalent substitution $(Zr^{4+} \rightarrow Ti^{4+})$, $x_{f-r} = 0.27$;
- for the heterovalent substitution $(Nb^{5+} + \frac{1}{2}\square \rightarrow (1/2)Ba^{2+} + Ti^{4+})$, $x_{f-r} = 0.06$;
- for both the anionic and cationic heterovalent substitutions $(Ti^{4+} + 3O^{2-} \rightarrow Li^+ + 3F^-)$, $x_{f-r} = 0.045$.

In this list, the homovalent Zr^{4+} ions are the softest defects while the doubles $Li^{3+} + 3F^-$ are the strongest.

The shape of the phase diagrams displayed in figures 3 and 4 for $Ba(Ti_{1-x}Zr_x)O_3$ and $Ba_{1-x/2}\square_{x/2}(Ti_{1-x}Nb_x)O_3$ respectively is also of interest. Indeed, for $x < x_{f-r}$, the paraelectric–ferroelectric transition temperature decreases on increasing x. When the crossover composition x_{f-r} is reached, this transition line splits because of the already mentioned dielectric dispersion in the relaxor state. The Vogel–Fulcher line can be considered, following equation (1), as the zero-frequency extrapolation of the various T_m lines. The error bars that are drawn on figures 3 and 4 take into account the limited accuracy of the Vogel–Fulcher fitting which mainly stems from the limited frequency range that we used. Nevertheless, we note that in lead-containing relaxors, extended frequency ranges usually lead to similar Vogel–Fulcher temperatures. Keeping in mind these limitations, the Vogel–Fulcher line $T_{VF}(x)$ $(x > x_{f-r})$ is the best extrapolation of the ferroelectric line $T_C(x)$ $(x < x_{f-r})$. This is the main experimental feature that will be discussed in the following.

4. Discussion

The Vogel–Fulcher line $T_{VF}(x)$ $(x > x_{f-r})$ and the ferroelectric transition line $T_C(x)$ $(x < x_{f-r})$ are aligned, suggesting a possible link between the ferroelectric and relaxor transitions.
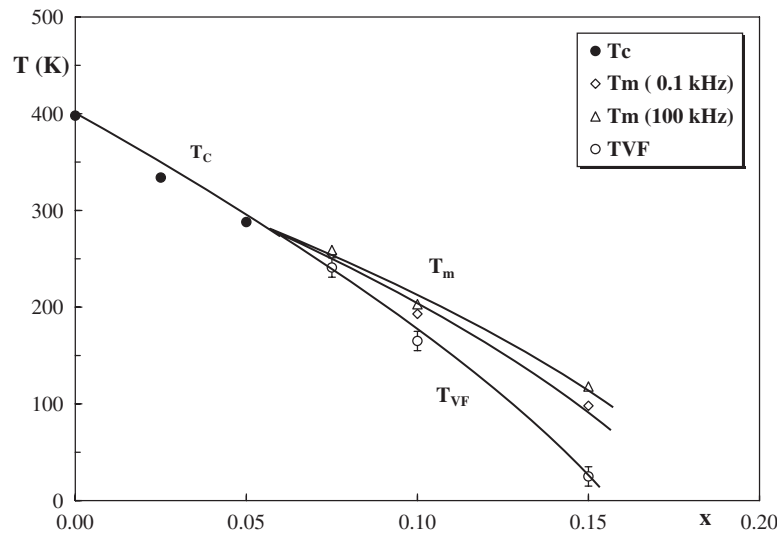
Figure 4. Variations of the transition temperatures T_C, T_m and T_{VF} with composition for ceramics of the $Ba_{1-x/2}\square_{x/2}(Ti_{1-x}Nb_x)O_3$ system.

This link is in no way obvious since these two states are very different in nature. In lead-containing relaxors, the interplay between ferroelectricity and the relaxor state displays a wealth of different features. In PMN, the ferroelectricity is always field induced and the transition temperature lies well below the relaxor transition. In PST and PSN, the ferroelectricity is spontaneous in chemically ordered compounds and closely follows the relaxor transition.

Having established a link between the relaxor and ferroelectric lines in our lead-free compounds, we need to understand the possible origin of this link. We first recall that the ferroelectric transition ($x < x_{f-r}$) follows a strong increase of the interaction (or correlation length) at T_C. In the following, we will call this optimal ferroelectric correlation length ξ_∞. In the real world, this correlation length is not infinite as it should theoretically be. We will not discuss here the possible occurrence of a limited correlation length for $T \gg T_C$, well into the paraelectric state. In the soft mode picture of $BaTiO_3$, the infinite correlation length at T_C results from the condensation of a phonon mode which mainly includes the Ti–O bond oscillations. An alternative model [15] takes into account correlated Ti–O chains which are present at all temperatures. In both these cases, the Ti–O bonds are the key source for ferroelectricity. These bonds are exactly what we disrupt on substituting Zr^{4+} for Ti^{4+}, Nb^{5+} for Ti^{4+} and Li^+–F^- for Ti^{4+}–O^{2-}. We recall that the perturbation strength ΔP is increasing when going from the former substitution to the latter. The ferroelectric line $T_C(x)$ for $x < x_{f-r}$ stems from a decrease of the maximal correlation length ξ_{max} as x increases which we can write as $\xi_{max} \propto \xi_\infty/x \Delta P$. Formally, this equation means that there are two ways to decrease the ferroelectric correlation length and thus to decrease the ferroelectric transition temperature: increase of the number of substituted defects x and increase of the strength of perturbation of each defect ΔP. The former parameter leads to the negative slope of $T_C(x)$ and the latter increases the slope of this line. This is qualitatively consistent with our observations in our three studied families. The next step is to consider that each substituted point defect perturbs a part of its surrounding host $BaTiO_3$ lattice. Because of the anisotropic nature of this lattice, such polarized clusters are expected to have an ellipsoid shape. Using the Ornstein–Zernicke formalism, one can think that this perturbation is exponentially decreasing along the radii of
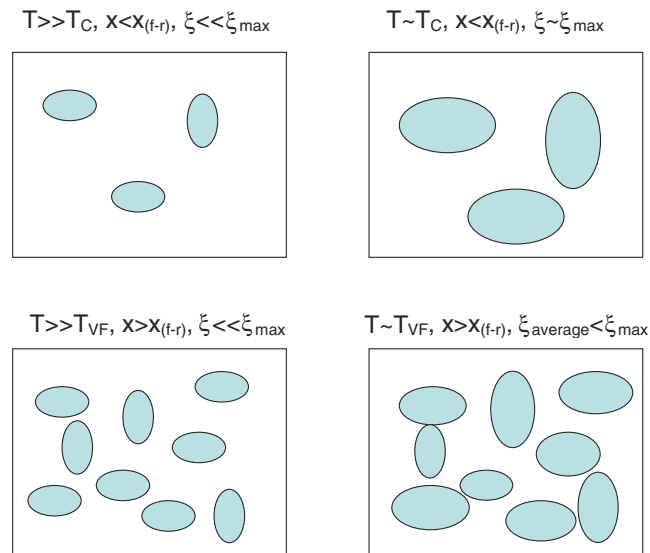
Figure 5. A sketch of the impurity induced clusters in the BaTiO$_3$ host lattice. On cooling to the transition temperature, the clusters can reach their maximum extension when their density is low, leading to a ferroelectric state (upper row). When their density is high, this optimal size cannot be reached and a distribution of cluster size sets in, leading to a relaxor state (lower row).

(This figure is in colour only in the electronic version)

these ellipsoids as $\Delta P \exp(-\frac{r}{\xi})$ [16]. It is beyond of the scope of the present paper (if not impossible) to exactly define this exponential decrease. What we can say is that the maximum size of these perturbed clusters is reached when $\xi = \xi_{max}$, i.e. at T_C. This is the key point: not only does the maximum correlation length ξ_{max} drive the host matrix properties, but also it sets the size of the perturbed clusters around each substituted defect. Since, in our assumption, ξ_{max} decreases both with increasing x and with increasing ΔP, the picture which arises is the following (figure 5):

- for $x < x_{f-r}$, the density of impurity induced clusters is very small and the BaTiO$_3$ host matrix properties are kept, with just a decrease of the maximal correlation length ξ_{max}; at the same time, each cluster can reach its maximum size (figure 5, upper row);
- when $x \sim x_{f-r}$ small clusters start to interact with each other; in this model, x_{f-r} is the 'right' point where all the macroscopic sample is filled by impurity induced microscopic clusters, and this interaction is the source for the observed dielectric dispersion;
- when $x > x_{f-r}$ the maximal correlation length cannot be reached and the Vogel–Fulcher temperature is the temperature where all clusters stop relaxing; the clusters can no longer reach their maximum size and, because of the interaction among clusters, a size distribution sets in (figure 5, lower row).

Without a quantitative evaluation of ΔP and $\xi(x)$, we cannot go further in the quantitative description of the ferroelectric–relaxor crossover. We can however explain why the ferroelectric and relaxor phase diagrams are aligned: this is simply because the BaTiO$_3$ ultimate correlation length ξ_∞ appears in all the spatial parameters that we defined. In other words, the BaTiO$_3$ correlation length is imprinted on both the matrix and cluster properties; the Ti–O bond oscillations are the key mechanisms. This picture is consistent with the one which was drawn up on the basis of high pressure Raman scattering experiments and which uses the BaTiO$_3$

correlation length. Also, we recall that the soft mode related cluster sizes and the Ornstein–Zernicke function were used in the case of lithium substituted $KTaO_3$ [17, 18]. Starting from these pioneering works, several attempts have been made to translate the cluster model to lead-containing relaxors. We feel that the continuous crossover that we have evidenced in lead-free compounds is strong evidence in favour of a cluster model of relaxors. However, the comparison between lead-containing and lead-free relaxors is limited since:

- a number of features of lead-containing relaxors do not appear in lead-free relaxors (diffuse scattering, high pressure induced Raman lines, . . .);
- the electronic lone pair of lead leads to very peculiar Pb dynamics which is not present in our Ba-based compounds;
- a continuous crossover from ferroelectric to relaxor states in Pb-based compounds is lacking; there is perhaps one example of such crossover which is in $PbTiO_3$:La for which x_{f-r} is about 0.20—however, this is very different from the case for standard relaxors where the substitution has single discrete values (0.33/0.66 or 0.50/0.50).

To summarize, we have evidenced a continuous crossover from ferroelectric to relaxor states in a number of lead-free perovskites with very different substitution types and levels. We suggest that both the host matrix and the impurity induced clusters are triggered by the $BaTiO_3$ soft mode correlation length.

References

[1] Ravez J and Simon A 1997 *C. R. Acad. Sci.* II **325** 481
[2] Cross L E 1994 *Ferroelectrics* **151** 305
[3] Ravez J and Simon A 1998 *J. Korean Phys. Soc.* **32** S955
[4] Ravez J and Simon A 1997 *Eur. J. Solid State Inorg. Chem.* **34** 1199
[5] Ravez J and Simon A 2000 *Solid State Sci.* **2** 525
[6] Barhi F, Khemakhem H, Simon A and Ravez J 2001 *Phys. Status Solidi* a **184** 459
[7] Ravez J and Simon A 2000 *Phys. Status Solidi* a **178** 793
[8] Khemakhem H, Simon A, von der Mühll R and Ravez J 2000 *J. Phys.: Condens. Matter* **12** 5951
[9] Kherfah A, Taïbi K, Guehria-Laïdoudi A, Simon A and Ravez J 2000 *Mater. Lett.* **42** 189
[10] Ravez J and Simon A 2001 *J. Solid State Chem.* **162** 260
[11] Kreisel J *et al* 2004 *Phys. Rev.* B at press
[12] Simon A and Ravez J 2004 *Solid State Sci.* **5** 1459
[13] Viehland D, Jang S J and Cross L E 1990 *J. Appl. Phys.* **68** 2916
[14] Glazounov A E and Tagantsev A K 1998 *Appl. Phys. Lett.* **73** 856
[15] Comes R, Lambert M and Guinier A 1968 *Solid State Commun.* **6** 719
[16] Levanyuk A P, Sigov A S and Sobyanin A A 1983 *Light Scattering Near Phase Transitions* ed H Z Cummins and A P Levanyuk (Amsterdam: North-Holland) chapter 3
[17] Vogt H 1990 *Phys. Rev.* B **41** 1184
[18] Vugmeister B E and Glinchuk M D 1990 *Rev. Mod. Phys.* **62** 4